

Arbitrary precision in multipath interferometry

Giacomo M. D'Ariano and Matteo G. A. Paris

Istituto Nazionale di Fisica della Materia, Sezione di Pavia, via Bassi 6, I-27100, Pavia, Italy

(Received 25 March 1996)

Interferometers with M paths are studied. It is shown that the accuracy of the phase-shift measurement can be improved by increasing the number of paths. For a detection scheme that uses coherent input states, phase sensitivity rescales as $\Delta\varphi \propto M^{-1}$, and nonunit quantum efficiency η at detectors only decreases the effective M by a factor $\sqrt{\eta}$. [S1050-2947(97)00701-4]

PACS number(s): 42.50.Lc, 03.65.Bz, 07.60.Ly

Interferometric detection allows us to measure tiny variations of the optical path of a light beam, corresponding to very small phase shifts of the radiation field. Even with conventional interferometers, such measurement is generally considered very accurate. However, in special situations, such as for detecting gravitational waves, a much more accurate measurement is needed [1]. The limit to the precision of the measurement is posed by the limited available amount of field energy, which, in the form of radiation pressure, perturbs the parameter that is monitored by the phase shift.

In conventional two-path Mach-Zehnder (or Michelson) interferometers that use coherent light, phase sensitivity is bounded by the so-called shot-noise limit

$$\Delta\varphi \propto \frac{1}{\sqrt{N}}, \quad (1)$$

where N is the mean photon number of the impinged radiation. A number of possible mechanisms have been analyzed for improving two-path interferometry [2–6]. Mostly, attention was focused on methods for achieving the ideal bound [7]

$$\Delta\varphi \propto \frac{1}{N} \quad (2)$$

by driving the interferometer with nonclassical states of light. Correlations between the photons in the two arms are produced, which are needed for beating the shot noise originated by the zero-point fluctuations at the input. After the earlier indication of using squeezed states to reduce quantum fluctuations [2], other proposals suggested to coherently drive the optical fields with correlated atomic transitions [3], or by active elements such as four-wave mixers [4]. More recently, suitable two-mode states [5] have been suggested as optimal inputs for approaching the Heisenberg limit (2) or, alternative to homodyne interferometry, a nonconventional heterodyne interferometer has been proposed that uses two-mode down-converted radiation [6].

In this paper we avoid using exotic states of light. Following the earlier suggestions of Ref. [8], we consider a multipath interferometric arrangement where a coherent input signal is split into many beams by a $2M$ -port multisplitter. As will be shown in the following, interference among an increased number M of available paths results in an improvement of the phase sensitivity according to the rescaling

$$\Delta\varphi \propto \frac{1}{\sqrt{NM}}. \quad (3)$$

This means that by increasing the number M of available paths, arbitrary precision in phase-shift measurements can be achieved with a *fixed amount* of energy impinged into the apparatus. It will also be shown that this interferometric scheme is only weakly affected by nonunit quantum efficiency at photodetectors.

Linear $2M$ -port optical couplers [9,10] are a generalization of standard lossless beam splitters. The M input modes a_i , $i=1, \dots, M$, are combined together, resulting in a new set of M output modes b_j , $j=1, \dots, M$. As for the beam splitter, which is described by a unitary 2×2 matrix [11], any lossless $2M$ -port multisplitter is characterized by a unitary $M \times M$ matrix [10] where each matrix element A_{ij} represents the transmission amplitude from the i th input port to the j th output port. The $2M$ -port multisplitter that is fully symmetrical among its ports is referred to as the *canonical multisplitter*. It is described by a unitary matrix \mathbf{A} whose elements depend only on the number M of modes and are just the M th complex roots of unity [10]

$$A_{kj} = \frac{1}{\sqrt{M}} \exp \left[\frac{2\pi i}{M} (k-1)(j-1) \right]. \quad (4)$$

These devices have been already implemented by single-mode optical fibers technology: commercial tritters ($M=3$) and couplers with higher M have been available for a long time [12]. In Ref. [13] it is also shown that any unitary M -dimensional matrix can be factorized into a sequence of two-dimensional transformation and thus any $2M$ -port multisplitter can be implemented by a suitable configuration of beam splitters. For example, the double-homodyne scheme of Ref. [14] is just the realization of a $M=4$ multisplitter homodyne detector

In Fig. 1 we report a schematic diagram of a multipath interferometer. The M input modes a_i , $i=1, \dots, M$ are mixed by the first $2M$ -port splitter, and then follow different optical paths corresponding to different phases ϕ_1, \dots, ϕ_M . Light beams are then recombined and the output modes from the second multisplitter are detected by M identical photodetectors. The interferometer is described by a transfer matrix $\mathbf{T}(\phi_1, \dots, \phi_M)$ whose dependence on the relative phases of the involved modes can be recast in the following canonical form:

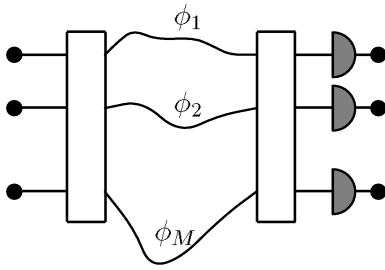


FIG. 1. Schematic diagram of a multipath interferometer.

$$\mathbf{T}(\phi_1, \dots, \phi_M) = \mathbf{A}\mathbf{V}(\phi_1, \dots, \phi_M)\mathbf{A}, \quad (5)$$

where the matrix \mathbf{A} is given in Eq. (4) and the phase shifts are contained in the matrix elements of \mathbf{V} ,

$$V_{kj}(\phi_1, \dots, \phi_M) = \exp(i\phi_k) \delta_{kj}, \quad (6)$$

δ_{kj} denoting the Kronecker delta. Explicitly, the transfer matrix of the interferometer is given by

$$T_{kj}(\phi_1, \dots, \phi_M) = \frac{1}{M!} \sum_{l=1}^M e^{i[\phi_l + (2\pi/M)(l-1)(k+j-2)]}. \quad (7)$$

The interferometer detects the commuting photocurrent $\hat{I}_n = b_n^\dagger b_n$, $n=1, \dots, M$, at the M outputs. The *in-out* evolution of field modes is given by

$$b_n = \sum_{l=1}^M T_{nl}(\phi_1, \dots, \phi_M) a_l, \quad [b_m^\dagger, b_n] = \delta_{mn}. \quad (8)$$

The probability distribution of the output photocurrents can be calculated as the multiple Fourier transform of a characteristic function

$$P(I_1, \dots, I_M) = \int_{-\pi}^{\pi} \frac{d\lambda_1}{2\pi} \dots \int_{-\pi}^{\pi} \frac{d\lambda_M}{2\pi} \prod_{k=1}^M \exp(-i\lambda_k I_k) \chi(\lambda_1, \dots, \lambda_M), \quad (9)$$

with the characteristic function $\chi(\lambda_1, \dots, \lambda_M)$ given by

$$\chi(\lambda_1, \dots, \lambda_M) = \text{Tr} \left\{ \hat{\rho}_{in} \prod_{k=1}^M \exp(-i\lambda_k b_k^\dagger b_k) \right\} \quad (10)$$

$$= \text{Tr} \left\{ \hat{\rho}_{out} \prod_{k=1}^M \exp(-i\lambda_k a_k^\dagger a_k) \right\}. \quad (11)$$

Equations (10) and (11) represent the characteristic function in the Heisenberg and Schrödinger pictures, respectively, with $\hat{\rho}_{in}$ and $\hat{\rho}_{out}$ denoting the density operator of the radiation state at the input and the output of the interferometer.

We now consider the standard interferometric configuration, in which one input is excited into a coherent state by a laser beam, whereas the other inputs are vacuum. The input state is represented by the state vector signal mode

$$|\Psi_{in}\rangle = |\alpha, 0, \dots, 0\rangle, \quad (12)$$

with mode a_1 in the coherent state $|\alpha\rangle$. As coherent states are eigenstates of the annihilation operator, their Schrödinger evolution is given by the same transfer matrix of the Heisenberg evolution of modes. Thus we can write the output state corresponding to the input (12) by means of Eq. (8) as follows:

$$|\Psi_{out}\rangle = |T_{11}\alpha, \dots, T_{M1}\alpha\rangle. \quad (13)$$

The characteristic function $\chi(\lambda_1, \dots, \lambda_M)$ can now be easily evaluated in the Schrödinger picture. Upon inserting Eq. (13) into Eq. (11) and then into Eq. (9) one obtains the output probability distribution of photocurrents

$$P(I_1, \dots, I_M) = \prod_{k=1}^M e^{-|\beta_k|^2} \frac{|\beta_k|^{2I_k}}{I_k!}, \quad (14)$$

where

$$|\beta_k|^2 = \langle \hat{I}_k \rangle = \langle \hat{\Delta I}_k^2 \rangle = |\alpha|^2 |T_{1k}(\phi_1, \dots, \phi_M)|^2. \quad (15)$$

The probability distribution is factorized into a product of Poisson distributions of each photocurrent. It is worth noticing that this result is not a mere consequence of commutation among output photocurrents, but also depends on the choice Eq. (12) for the state at the input.

The influence of relative phases on the output photocurrents can be used for a number of tasks. Here we focus attention on monitoring a fixed phase shift φ among contiguous paths (a general analysis will be reported elsewhere). The relative phase shifts are given by

$$(\phi_{k+1} - \phi_k) = \varphi, \quad k=1, \dots, M-1. \quad (16)$$

After replacing this choice into Eq. (7) the modulus of the relevant matrix elements $|T_{1k}(\varphi, 2\varphi, \dots, M\varphi)|^2 \equiv F_M^k(\varphi)$ of the transfer matrix are given by

$$F_M^k(\varphi) = \frac{1}{M^2} \frac{1 - \cos[M(\varphi + \theta_k)]}{1 - \cos(\varphi + \theta_k)}, \quad (17)$$

where $\theta_k = 2\pi/M(k-1)$, $k=1, \dots, M$. The functional dependence versus φ in Eq. (17) is identical for all photocurrents, with just an additional shift θ_k . We now consider only one photocurrent, in order to find the optimal working regime for phase detection. Optimization could be obviously repeated for each photocurrent; however, the final result will be just a set of M equivalent optimal configurations.

Let us consider now a given fixed phase shift φ between contiguous paths. By choosing the mean value (15) as *phase estimator*, each random outcome I_1 of the first photocurrent corresponds to an estimate φ_* obtained by inverting Eq. (17) as follows:

$$\varphi_* = [F_M^1]^{-1} \left(\frac{I_1}{|\alpha|^2} \right). \quad (18)$$

The behavior of $F_M^1(\varphi)$ as a function of φ is reported in Fig. 2 for various values of M . It can be usefully inverted in the first branch $\varphi \in [0, 2\pi/M]$, which represents the region that is explored by the interferometer. A photocurrent outcome I_1 contains information on phase φ if it is smaller than $\mathcal{I}_{max} = |\alpha|^2$ and larger than the threshold value \mathcal{I}_{min} that corresponds to the height of the second maximum of $F_M^1(\varphi)$. From Fig. 2 it is apparent that the value of \mathcal{I}_{min} rapidly

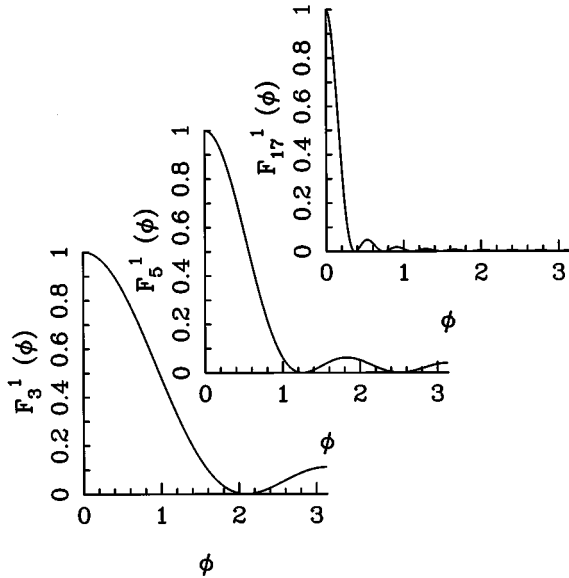


FIG. 2. The function $F_M^1(\phi)$ for increasing values of M . The number of oscillations increases and their height vanishes.

decreases versus M , and thus the number of discarded data becomes negligible for large M . For not too low intensities at the input, the estimates φ_* are distributed around $[F_M^1]^{-1}(|\beta_1|^2/|\alpha|^2) \equiv \varphi$, with a variance given by

$$\Delta\varphi \equiv \sqrt{\langle \Delta I_1^2 \rangle} \left| \frac{\delta \langle \hat{I}_1 \rangle}{\delta \varphi} \right|^{-1} = \frac{1}{2|\alpha|} \left[\frac{\delta \sqrt{F_M^1(\varphi)}}{\delta \varphi} \right]^{-1} \quad (19)$$

$$= \frac{M}{|\alpha|} \tan \frac{\varphi}{2} \frac{\sqrt{(1 - \cos \varphi)[1 - \cos(M\varphi)]}}{|M \sin(M\varphi) \tan(\varphi/2) + \cos(M\varphi) - 1|},$$

which represents the phase sensitivity of the interferometer. As it is apparent from Eq. (19), the accuracy in monitoring the phase shift depends on the phase value itself. The optimal working point φ_{WP} for the interferometer corresponds to the minimum points of $\Delta\varphi$. For two and three paths interferometers the minimization procedure can be carried out analytically. We have

$$\varphi_{WP}^{(2)} = \pi, \quad \Delta\varphi_2 = \frac{1}{|\alpha|}, \quad (20)$$

$$\varphi_{WP}^{(3)} = \frac{\pi}{2}, \quad \Delta\varphi_3 = \frac{3}{4} \frac{1}{|\alpha|}. \quad (21)$$

The results in Eq. (20) correspond to the Mach-Zehnder two-path interferometer, whose sensitivity is bounded by the customary shot-noise limit. Equation (21) shows that for a three-path interferometer the proportionality constant improves. This agrees with earlier experimental results [15] obtained for a classical Mach-Zehnder-like three-path interferometer. Equation (21) is also in agreement with the results of Ref. [16], where the experimental realization of an *all-fiber* three-path interferometer was reported. In the general case $M \geq 4$ the optimization procedure can be easily performed numerically. The absolute minimum of sensitivity $\Delta\varphi_M$ in Eq. (19) is given by

$$\varphi_{WP}^{(M)} \approx \frac{A}{M}, \quad \Delta\varphi_M \approx \frac{1}{|\alpha|} \frac{A-2}{M}, \quad (22)$$

where A is a numerical constant (from a best fit valid for $4 \leq M \leq 1000$ we obtained $A \approx 4.17$). The absolute minimum is always contained in the first branch of $[F_M^1]^{-1}(I_1)$. Notice that no further improvement in sensitivity can be obtained by considering also the $M-1$ remaining photocurrents because the working point for I_1 corresponds to unuseful branches for the other photocurrents.

Equation (22) is the central result of the present paper. It shows that phase sensitivity can be improved at will by just increasing the number of paths of the interferometer. There are now two different kinds of scaling. On the one hand, there is shot-noise scaling versus the input energy due to the quantum fluctuations at unused ports of the interferometer. On the other hand, one has a rescaling versus the number of paths into which the input field is split. This means that for a fixed amount of energy impinged into the interferometer the phase sensitivity can be arbitrarily improved by just increasing the number of paths. The available phase region $[0, 2\pi/M]$ that can be explored by the multipath interferometer decreases versus the number of paths. However, the ratio between this range and the phase sensitivity (22) remains constant, leading to a significant improvement in monitoring small phase shifts. Thus, there are no fundamental limitations on accuracy when measuring small phase shifts by multipath interferometers, and there is only the technical problem of realizing higher M multipoint linear couplers.

In Fig. 3 we report results from numerical simulations of interferometric detections. We consider interferometers supplied by the same coherent beam with amplitude $|\alpha| = 10$ and a different number of paths. The distributions of a sample of 10^4 random outcomes for the photocurrent I_1 is reported for the optimal configuration and after a phase shift $\varphi = 10^{-2}$ rad. The amplifying effect of the increasing number of paths is apparent: the two (shifted and unshifted) distributions would have been almost undistinguishable if measured by a two-path Mach-Zehnder interferometer. Here we do not analyze the very low signal regime $|\alpha| \approx 1$, when the distribution of the estimates φ_* (18) results in only a few spaced peaks: this situation, however, could be of interest in improving a phase communication channel.

Let us now consider the effect of nonunit quantum efficiency η at photodetectors. The probability distributions of photocurrents become a Bernoulli convolutions of the ideal distributions. The output photocurrents are still Poisson distributed, however, with mean value multiplied by η . Upon substituting this result into the first of Eqs. (19), the phase sensitivity at the working point $\varphi_{WP}^{(M)}$ is given by

$$\Delta\varphi_{M\eta} = \frac{1}{|\alpha|} \frac{1}{M\sqrt{\eta}} \equiv \Delta\varphi_M \frac{1}{\sqrt{\eta}}, \quad (23)$$

with $\Delta\varphi_M$ given by Eq. (22). Equation (23) shows that inefficient detection results only in a slight deterioration of the numerical constant, without affecting the inverse scaling versus the number of paths: one has just a decrease of the effective number of paths by a factor $\sqrt{\eta}$. We thus conclude that the present multipath interferometric scheme can be very

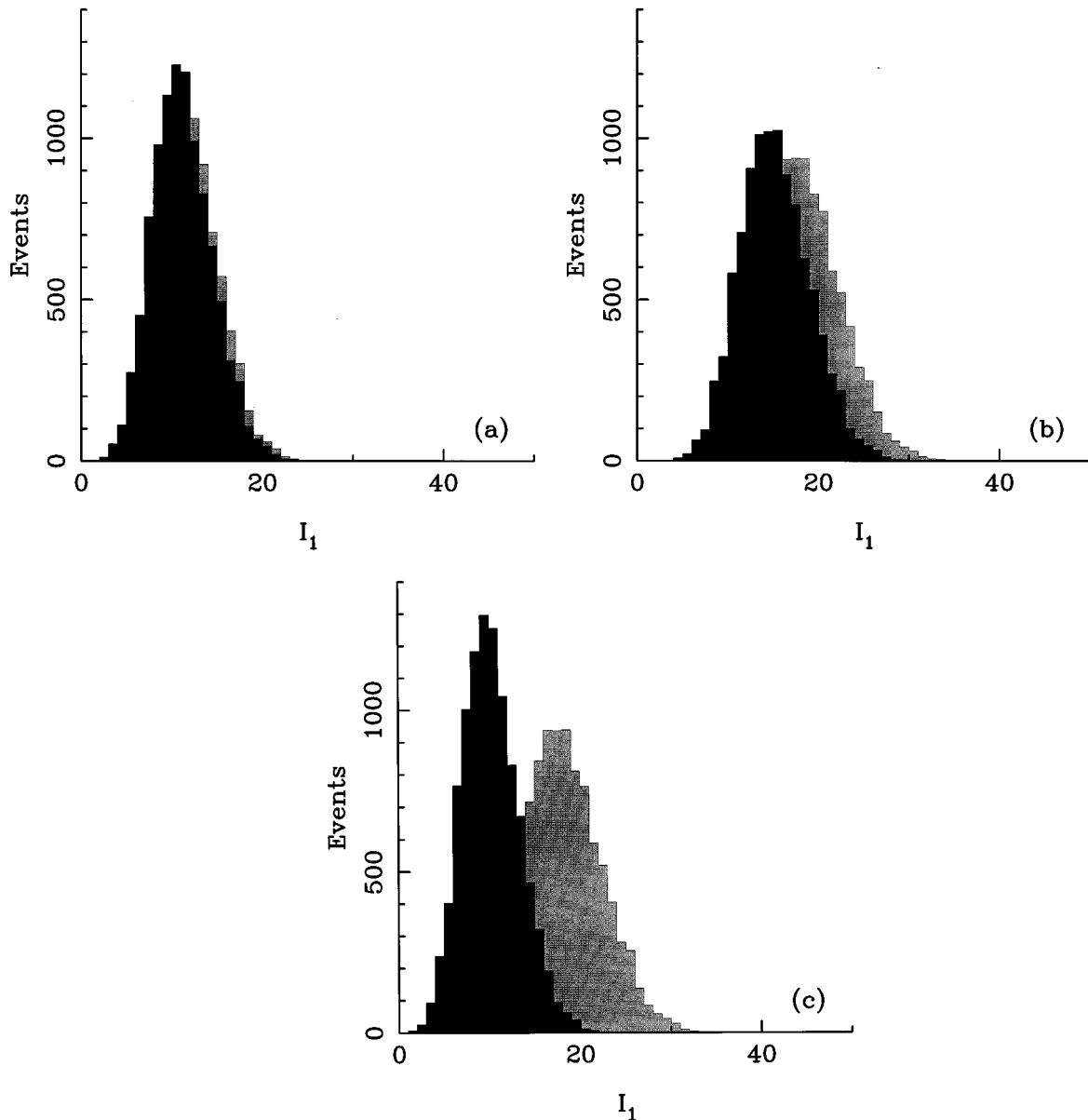


FIG. 3. Numerically simulated interferometric detection. Experimental distributions of a sample of 10^4 random outcomes of the photocurrents I_1 are reported for the interferometer at the working point and after a shift of 10^{-2} rad. Results for an (a) $M=3$, (b) $M=17$, and (c) $M=50$ interferometer. The input signal is always a coherent state with average photon number $|\alpha|^2=100$. The amplifying effect of the increasing number of paths is apparent.

effective in practice because it is not affected by inefficient detection. This is in contrast to the case of interferometry that uses nonclassical light, where inefficient photodetection strongly degrades sensitivity [17], as losses always hinder detection of any nonclassical effect.

In conclusion, a highly sensitive interferometric scheme based on multisplitter linear couplers has been presented. Such interferometers can be implemented both as *all-fiber*

devices and by discrete optical components. The increasing number M of paths makes the interferometer more sensitive, with sensitivity linearly improving versus M , thus providing a way to achieve arbitrary precision at a fixed amount of energy impinging into the apparatus. Nonunit quantum efficiency of photodetectors does not affect the scaling law versus M , and is just equivalent to consider a slightly lower effective number of paths.

[1] K. Thorne, Rev. Mod. Phys. **52**, 285 (1980); W. W. Chou, *ibid.* **57**, 61 (1985).

[2] C. M. Caves, Phys. Rev. D **23**, 1693 (1981).

[3] M. O. Scully, Phys. Rev. Lett. **55**, 2802 (1985).

[4] B. Yurke, S. L. McCall, and J. R. Klauder, Phys. Rev. A **33**, 4033 (1986).

[5] B. C. Sanders and G. J. Milburn, Phys. Rev. Lett. **75**, 2944 (1995).

- [6] G. M. D'Ariano and M. Sacchi, *Phys. Rev. A* **52**, R4309 (1995).
- [7] G. M. D'Ariano and M. G. A. Paris, *Phys. Rev. A* **49**, 3022 (1994).
- [8] F. Zernike, *J. Opt. Soc. Am.* **40**, 326 (1950).
- [9] N. G. Walker, *J. Mod. Opt.* **34**, 15 (1987).
- [10] K. Mattle, M. Michler, H. Weinfurter, A. Zeilinger, and M. Zukowski, *Appl. Phys. B* **60**, S111 (1995).
- [11] R. A. Campos, B. E. A. Saleh, and M. C. Teich, *Phys. Rev. A* **42**, 4127 (1990).
- [12] S. K. Sheem, *J. Appl. Phys.* **52**, 3865 (1981).
- [13] M. Reck, A. Zeilinger, H. J. Bernstein, and P. Bertani, *Phys. Rev. Lett.* **73**, 58 (1994).
- [14] J. W. Noh, A. Fougères, and L. Mandel, *Phys. Rev. Lett.* **67**, 1426 (1991).
- [15] P. Hariharan and D. Sen, *J. Sci. Instrum.* **36**, 70 (1959).
- [16] G. Weihs, M. Reck, H. Weinfurter, and A. Zeilinger, *Opt. Lett.* **21**, 302 (1996). Here a different definition of sensitivity is used, which does not account for fluctuations in the measured photocurrents. However, this leads to the same working point of Eq. (21), with only a negligible quantitative disagreement with respect to our estimated sensitivity.
- [17] M. G. A. Paris, *Phys. Lett. A* **201**, 132 (1995); G. M. D'Ariano, M. G. A. Paris, and R. Seno, *Phys. Rev. A* **54**, 4495 (1996).